Field dependence of μSR signals in a polycrystalline magnet

2007 J. Phys.: Condens. Matter 19 456207

(http://iopscience.iop.org/0953-8984/19/45/456207)

IOP PUBLISHING JOURNAL OF PHYSICS: CONDENSED MATTER

J. Phys.: Condens. Matter **19** (2007) 456207 (11pp) doi:10.1088/0953-8984/19/45/456207

Field dependence of μSR signals in a polycrystalline magnet

F L Pratt

ISIS Facility, Rutherford Appleton Laboratory, Chilton, Oxfordshire OX11 0QX, UK

Received 17 August 2007, in final form 21 September 2007
Published 11 October 2007
Online at stacks.iop.org/JPhysCM/19/456207

Abstract

Studies of magnetically ordered materials using implanted muons usually focus on the behaviour of the muon polarization in zero applied magnetic field, where precession signals reflect the static internal fields that appear in the magnetically ordered state. In many cases the magnetic behaviour under applied magnetic field is also of interest. However, detailed analysis and interpretation of field-dependent μSR signals requires a clear understanding of the different types of behaviour that may be expected following various possible responses of the spin distribution to the applied field. In order to aid such investigations, quantitative analytical expressions are provided here for polycrystalline systems describing the behaviour of the muon polarization components and the precession frequency distribution in an applied field, under the initial assumption that the magnetic sublattices are not significantly perturbed by the applied field. Given these expressions, departures from this simple unperturbed behaviour can then be identified and interpreted in terms of the actual magnetic response to the applied field. An example is given using this approach in the analysis of a metamagnetic transition in a layered molecular magnet.

1. Introduction

The implanted muon has often been exploited as a local probe of magnetic systems [1, 2]. Studies usually focus on the behaviour of the muon polarization in zero applied field (ZF), since the observation of zero field precession signals can give unambiguous evidence for the presence of an internal field due to the onset of magnetic order. Besides these zero field studies, it can also be very useful to study the muon polarization behaviour under applied magnetic fields, in order to provide further information about the magnetic state and study any changes that take place in response to the applied field. Data in finite fields can also provide a useful consistency check on the interpretation of zero field data. However, previous applied field studies have generally only been rather qualitative due to the lack of a clear framework on which to base more quantitative studies. The present work therefore aims to fill this gap.

0953-8984/07/456207+11$30.00

The behaviour of the muon spin in this problem is described as a function of time t by the longitudinal muon spin polarization function $G_z(t)$, which gives the evolution of a muon spin initially polarized in the z direction, normalized so that $G_z(0) = 1$. For a magnetically ordered state in a ideal system with a unique muon site in zero externally applied field, the magnitude of the internal field seen by the muon takes the single value B_0. The polarization function $G_z(t)$ then contains a single oscillating component with amplitude $A_{\rm osc}$ and precession frequency $\omega = \gamma_\mu B_0$, where $\gamma_\mu = 2\pi \times 135.5$ MHz T^{-1} is the muon gyromagnetic ratio, along with a non-precessing component with amplitude A_z:

$$G_z(t) = A_z + A_{\rm osc} \cos \omega t. \tag{1}$$

The specific case of a randomly oriented polycrystalline magnet is considered here. This is the most common experimental sample configuration in μSR. In this case the internal field vector is distributed uniformly over a sphere with radius B_0, A_z takes the value $1/3$ and $A_{\rm osc}$ takes the value $2/3$, reflecting the orientationally averaged projection of the internal field distribution onto longitudinal and transverse components with respect to the initial muon polarization direction z. The behaviour once a finite external magnetic field is applied is however a rather more complex, problem and quantifying the expected behaviour in typical experimental situations is the subject of this paper.

In real magnetic systems there is always some broadening of the distribution of internal fields due to disorder and the effects of domain structure. Changes in the zero field muon relaxation function produced by this broadening have been reported in several previous studies, where such broadening is a dominant feature of the relaxation [3–5]. In this study we approach from the opposite limit where the broadening of the internal field distribution due to disorder is insignificant compared to the intrinsic 'geometrical' broadening produced by imposing an externally applied field. To reflect disorder-related broadening, a distribution of B_0 can be reintroduced into the equations we will derive as a final stage, thus allowing both intrinsic and extrinsic sources of broadening to be included. Likewise, the effects of finite dynamical spin fluctuations can be reintroduced to our final results as an additional contribution to the relaxation, with an associated contribution to the spectral broadening. Finally, it should also be noted that there may be a further contribution to the internal field distribution from nuclear dipolar fields; however, this is usually very much smaller than the electronic contribution and any associated broadening will be insignificant compared to the intrinsic and extrinsic effects related to the electronic spins.

2. Fixed spin system

The first situation to consider is the simplest possible case, where the effect of the field on the internal magnetic structure is insignificant as far as a muon measurement is concerned and can safely be ignored. This will generally be the case for weak applied fields where the magnetic anisotropy of the material is the dominant factor defining the sublattice orientation. A single implantation site is considered initially and the two cases of field orientation, longitudinal and transverse to the initial muon spin polarization, are considered in turn.

2.1. Longitudinal field

When a longitudinal field (LF) is applied, the total internal field at a particular site is the vector sum of B, the field applied externally along the axis z and the effective field from the ordered moments B_0, which has a single value but is randomly oriented in the polycrystalline powder

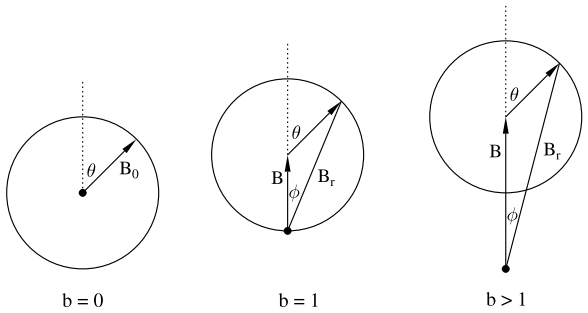

Figure 1. Effect of external longitudinal field B applied along the z axis on the resultant internal field B_r for a muon site where the internal field contribution from the magnetic order has magnitude B_0 at angle θ to the z axis. The dots shows the origin of the internal field distribution in each case and the circle represents a sphere describing the distribution of field contributions from magnetic order in randomly oriented crystallites of a polycrystalline array.

sample, making an angle θ to the longitudinal axis z (figure 1). The resultant magnitude of the internal field B_r seen by the muon has the value

$$B_r = \sqrt{B^2 + B_0^2 + 2B_0 B\cos\theta}. \tag{2}$$

Lower case notation will be used in the following to indicate fields normalized to B_0 and frequencies normalized to $\gamma_\mu B_0$, i.e. $b = f = B/B_0$ and $b_r = B_r/B_0$; (2) then becomes

$$b_r = \sqrt{b^2 + 1 + 2b\cos\theta}. \tag{3}$$

The angle ϕ between b_r and the longitudinal axis given by

$$\cos^2\phi = \frac{(b+\cos\theta)^2}{(b+\cos\theta)^2 + (\sin\theta)^2}. \tag{4}$$

The longitudinal polarization A_z is obtained by taking the orientational average of (4) with respect to θ

$$A_z = \overline{\cos^2\phi} = \int_0^\pi \frac{\sin\theta}{2}\,\mathrm{d}\theta\,\frac{b^2 + 2b\cos\theta + \cos^2\theta}{b^2 + 2b\cos\theta + 1}. \tag{5}$$

The remaining fraction of the polarization A_{osc} is transverse to the resultant field and provides the precession component. Evaluating the polarization integral (5) leads to the following functional forms for the two components against field:

$$A_z(b) = \frac{3}{4} - \frac{1}{4b^2} + \frac{(b^2-1)^2}{8b^3}\log\left|\frac{b+1}{b-1}\right| \tag{6}$$

and

$$A_{\mathrm{osc}}(b) = 1 - A_z(b). \tag{7}$$

The expression (6) for the longitudinal repolarization was originally reported by Satooka *et al* [6], although it should be noted that their intermediate expression was printed incorrectly; an earlier statement of it by Maruta *et al* [7] also had a misprint in the second term. The behaviour of (6) is shown in figure 2. Note that at the field where $b = 1$ the absolute polarization reaches $1/2$, whereas the midpoint of the polarization recovery is actually at a field value that is somewhat higher and close to $b = 4/3$. The width of the repolarization is also significantly narrower than the type of repolarization seen, for example, when decoupling the elements of

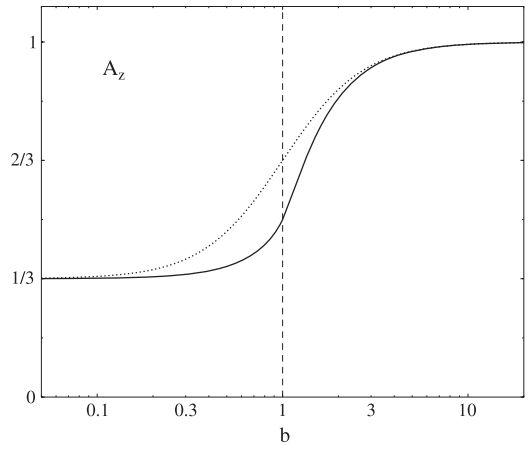

Figure 2. Dependence of A_z on longitudinal field b for a polycrystalline ordered magnet (solid line). The dotted line shows for comparison a quadratic-type decoupling function $1/3+2/3(b^2/(1+b^2))$.

the hyperfine tensor in muonium-type states [8], which usually contain terms taking a quadratic decoupling form such as $b^2/(1+b^2)$; these clearly decouple more slowly than (6) (see figure 2).

Turning to the precession component, it is clear that following (7) the precession amplitude will fall with field as the longitudinal component increases. It is also of interest to see how the muon precession frequency distribution changes as the external field increases. The mean of the frequency distribution seen by the muon $f_{\rm ave}$ $(=b_{\rm ave})$ and its RMS width $f_{\rm rms}$ $(=b_{\rm rms})$ can be calculated in a similar manner to the polarization, with the contributions to the field averages being weighted by the precession amplitude, which follows $\sin^2\phi$, giving

$$f_{\rm ave} = b_{\rm ave} = \frac{\int_0^\pi {\rm d}\theta\ \sin\theta\ \sin^2\phi\, b_r}{\int_0^\pi {\rm d}\theta\ \sin\theta\ \sin^2\phi}, \tag{8}$$

$$f_{\rm rms}^2 = b_{\rm rms}^2 = \frac{\int_0^\pi {\rm d}\theta\ \sin\theta\ \sin^2\phi\, b_r^2}{\int_0^\pi {\rm d}\theta\ \sin\theta\ \sin^2\phi} - f_{\rm ave}^2. \tag{9}$$

After performing the integrations, the following analytical expressions are obtained:

$$f_{\rm ave} = \frac{16}{15}\frac{P}{Q}, \tag{10}$$

$$f_{\rm rms}^2 = \frac{32b^3}{3Q} - f_{\rm ave}^2 \tag{11}$$

with

$$Q = 4b(1+b^2) - 2(1-b^2)^2 \log\left|\frac{b+1}{b-1}\right| \tag{12}$$

and

$$\begin{aligned} P &= 10b^3 - 2b^5 \qquad 0 \leqslant b < 1 \\ &= 10b^2 - 2 \qquad b > 1. \end{aligned} \tag{13}$$

When $b = 1$, $f_{\rm ave} = 16/15$ and $f_{\rm rms} = \sqrt{44}/15$. The behaviour of the resultant internal field parameters given by (10) and (11) is shown in figure 3, together with the amplitudes of the longitudinal and transverse components given by (6) and (7). A remarkably sharp change in the field-dependent behaviour of $f_{\rm ave}$ and $f_{\rm rms}$ is seen to take place around $b = 1$. In the high field limit $f_{\rm ave} \to b$ and $f_{\rm rms} \to 1/\sqrt{5}$.

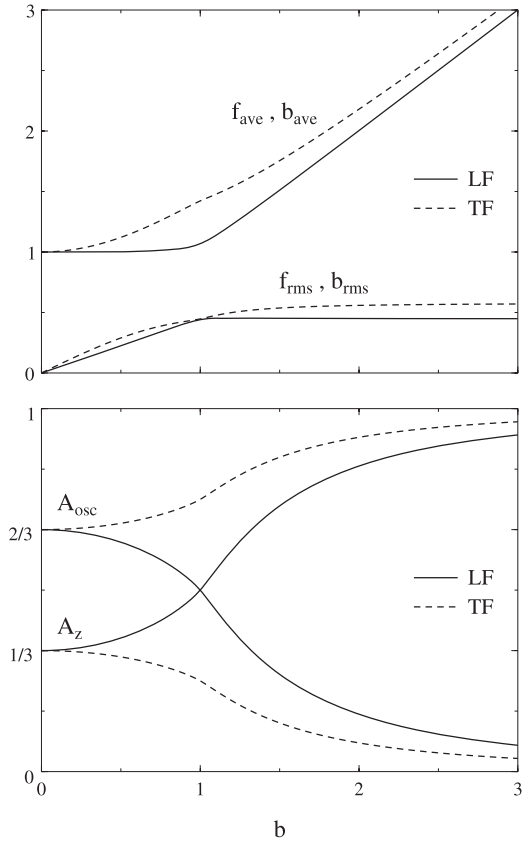

Figure 3. Field-dependent properties of the muon signal in a polycrystalline ordered magnet, described by (6)–(19). The upper plot shows the parameters of the precession frequency distribution and the lower plot shows the relative amplitudes of the transverse (precessing) and longitudinal (non-precessing) components $A_{\rm osc}$ and A_z. The field direction is either parallel (LF) or perpendicular (TF) to the initial muon spin direction.

2.2. Transverse field

When the field is applied in the transverse orientation, i.e. perpendicular to the initial muon spin direction z rather than parallel to it (TF case), the calculation is a little more complicated, as one no longer has the benefit of axial symmetry for performing the orientational averaging. Analytical expressions of similar form to the longitudinal ones can nevertheless still be obtained. The expressions for the polarization components are

$$A_z(b) = \frac{1}{8} + \frac{1}{8b^2} - \frac{(b^2-1)^2}{16b^3}\log\left|\frac{b+1}{b-1}\right| \tag{14}$$

and

$$A_{\rm osc}(b) = 1 - A_z(b). \tag{15}$$

The frequency distribution parameters are

$$f_{\rm ave} = b_{\rm ave} = \frac{16}{15}\frac{P}{Q} \tag{16}$$

and

$$f_{\rm rms}^2 = b_{\rm rms}^2 = \frac{32b^5 + 64b^3/3}{Q} - f_{\rm ave}^2 \tag{17}$$

with

$$Q = 4b(7b^2 - 1) + 2(1 - b^2)^2 \log\left|\frac{b+1}{b-1}\right| \tag{18}$$

and

$$\begin{aligned} P &= 12b^5 + 20b^3 \qquad 0 \leqslant b < 1 \\ &= 30b^4 + 2 \qquad b > 1. \end{aligned} \tag{19}$$

When $b = 1$, $f_{\rm ave} = 64/45$ and $f_{\rm rms} = \sqrt{404}/45$. The behaviour of the resultant internal field parameters given by (16) and (17) is shown as dashed lines in figure 3, together with the amplitudes of the longitudinal and transverse components given by (14) and (15). In the high field limit one finds again that $f_{\rm ave} \to b$, although the approach is slower than in the longitudinal case, and $f_{\rm rms} \to 1/\sqrt{3}$, a factor of $\sqrt{5/3}$ larger than for the longitudinal case. It is notable that the change in the field-dependent behaviour of $f_{\rm ave}$ and $f_{\rm rms}$ around $b = 1$ is much less sharp in the TF case than in the LF case.

2.3. Precession spectra and relaxation functions

Whereas relatively simple expressions can be derived for A_z, $A_{\rm osc}$ and the moments of the precession frequency spectrum, as has been shown in the previous two sections, full analytical expressions for the relaxation functions in the general case are rather cumbersome and the relaxation functions are best evaluated by numerical integration. In contrast to the relaxation functions, the precession frequency spectra can be expressed relatively simply: for the LF case the spectral intensity $S(b_r, b)$ of the precession signal is given for finite b by

$$S(b_r, b) = \frac{b_r^2 - (b + \cos\theta)^2}{2b_r b} \qquad |b - 1| < b_r < b + 1 \tag{20}$$

with $\cos\theta$ given by (3) and $S(b_r, b) = 0$ outside this range. The corresponding field-dependent relaxation function $G_z(t, b)$ is then given by

$$G_z(t, b) = A_z(b) + \int S(b_r, b)\cos(\gamma_\mu b_r t)\,{\rm d}b_r, \tag{21}$$

where $A_z(b) = \int(1 - S(b_r, b))\,{\rm d}b_r$ evaluates to (6) and the t scale is measured in units of the precession period at $b = 0$. The resulting behaviour is illustrated in figure 4. It can be seen that the distribution is quite symmetric except near $b = 1$. The extrema of the distribution have zero spectral weight, as the resultant field there is parallel to z. From the behaviour seen in figure 4 it is expected that a Gaussian function would provide a reasonably good first approximation to the spectrum and to the damping envelope of the precession signal.

For the TF case the precession frequency spectrum takes a rather different form

$$S(b_r, b) = \frac{b_r^2 - (1 - \cos^2\theta)/2}{2b_r b} \qquad |b - 1| < b_r < b + 1 \tag{22}$$

and the relaxation function is derived by substituting equations (14) and (22) in (21). As can be seen in figure 5 the spectrum shows a distinct splitting at lower fields and an asymmetric distribution as b increases, weighting the higher field side more strongly than the lower field side. In contrast to the LF case, the extrema of the distribution have a high spectral weight. The asymmetry of the spectrum starts to decrease again for $b > 1$ and at very high b the spectrum will tend towards a uniform top-hat function.

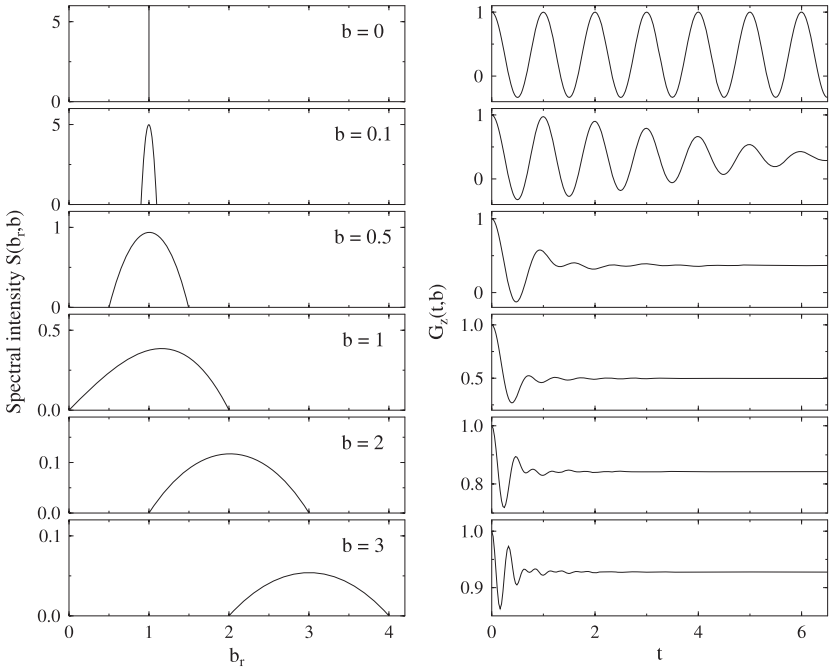

Figure 4. Evolution of the precession frequency spectrum and corresponding relaxation function with longitudinal applied field.

2.4. Discussion

Under the typical μSR experimental conditions of limited counting statistics and finite spectral broadening it may be difficult to resolve clearly the spectral features discussed in section 2.3; however, the ratio of the precessing and non-precessing components and the first moment of the precession frequency distribution derived in sections 2.1 and 2.2 can be measured more accurately and should be relatively robust against such experimental constraints. These parameters are therefore likely to provide the best way to detect changes in the spin distribution under applied field, which is the underlying motivation of this study; this will be discussed in the following section. Another aspect of real experimental systems is that there are often several muon sites and if the internal fields B_i at these sites are sufficiently different then a number of repolarization terms like (6) will be resolvable, as was demonstrated in measurements reported by Maruta *et al* [7]. If the B_i are relatively close then the contributions may not be individually resolved and a single repolarization feature will occur, but it will be broader than a single term described by (6). Similarly, a broadening is expected if the magnetic state itself contains significant disorder and a repolarization that is broader than predicted by (6) may be an indication of the presence of such a magnetic state. In principle for the fixed sublattice case the distribution of internal fields may be reconstructed from the measured repolarization behaviour using knowledge of the functional form (6) of A_z, i.e.

$$A_z^{\mathrm{ave}}(B) = \int A_z(B/B')p(B')\,\mathrm{d}B', \tag{23}$$

where $A_z^{\mathrm{ave}}(B)$ is the measured longitudinal polarization and $p(B')$ describes the internal field distribution before the application of the field B. This provides a complement to the direct use of spectral analysis methods on the precession signal. In the case of a study made at a

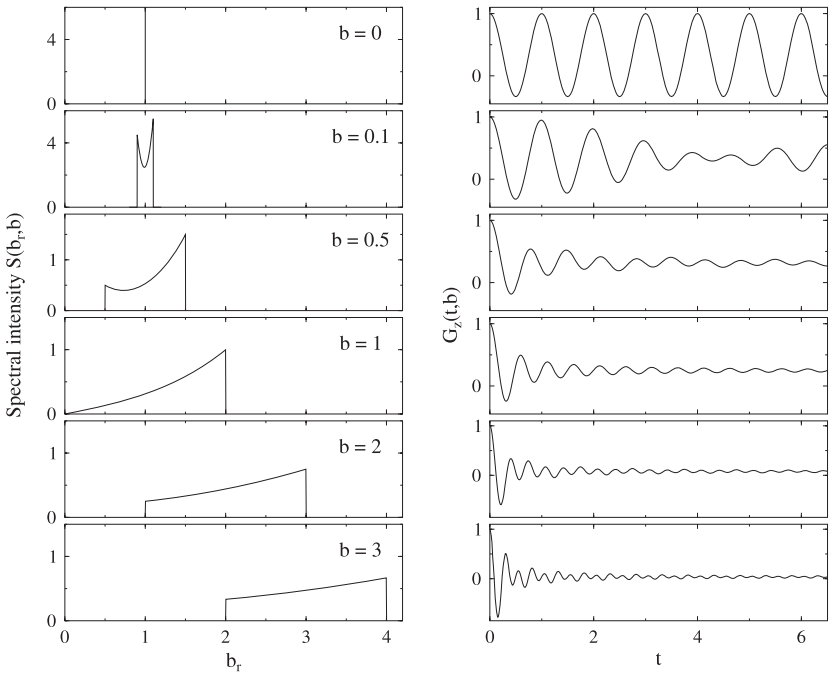

Figure 5. Evolution of the precession frequency spectrum and corresponding relaxation function with transverse applied field.

pulsed muon facility such as ISIS, some of the precession signals may in any case lie beyond the accessible frequency response of the instrument and this decoupling technique provides an alternative method of obtaining information about any muon sites with large associated internal fields that may be present, without the need to observe their precession signals directly.

3. Field-perturbed spin system

Having established the basic behaviour expected for the case where the magnetic spin system is not significantly perturbed by the fields applied in a muon study, it is now possible to explore the type of behaviour expected where the arrangement of the ordered spin system is modified by the applied field. This will, for example, happen where one is working with a relatively soft magnetic system and the fields that can typically be applied in the muon spectrometer may be sufficiently large to also produce significant changes in the orientational distribution of the magnetic moments themselves, for example by rotation and resizing of magnetic domains in the ferromagnetic case or by producing a spin-flop or spin-flip type transition in the antiferromagnetic case. Here the exact effect on the muon polarization would depend on the precise details of the magnetic structure, the muon site and the type of coupling of the muon to the magnetic spin system. In nearly all cases however, information about changes occurring in the magnetic state will be obtainable from comparing the actual measured precession frequency and polarization amplitude behaviour to the ideal reference case described in the previous section by equations (6)–(19), which describe the behaviour when the magnetic moments are fixed in their zero applied field configuration. For field-perturbed spins, the type of behaviour to be expected and the best way to monitor it can be considered for two general

cases, dependent on whether the major changes in the spin distribution take place for applied fields above or below the original internal field B_0, i.e. whether $b < 1$ or $b > 1$.

3.1. Transition for $b < 1$

The precession signal in LF mode would appear to be the best probe of the magnetic state when the change in the spin configuration occurs for $b < 1$, since the precession frequency still has large amplitude in this field range and shows hardly any intrinsic field dependence (figure 3). Quite subtle changes in the spin structure should be observable under these conditions, revealed by departures of the frequency and amplitude of the precession signal from the static behaviour, which is almost constant in this regime.

3.2. Transition for $b > 1$

When a spin transition takes place in the $b > 1$ high field region then the precession signal for TF configuration would appear to be the best probe, as it has a relatively large amplitude in this region (figure 3). However, studies at a pulsed facility such as ISIS may run into frequency response limitations at high fields and in this case we expect that monitoring of the non-precessing component A_z in LF mode, which can be done very accurately at a pulsed facility, would then provide the best way of detecting and studying the spin transition.

3.3. An experimental example

An example of a low-field spin transition measured by μSR at ISIS in the antiferromagnetic bilayer system $CuW(CN)_8(tetrenH_5)_{0.8}\cdot 7H_2O$ [9] is shown in figure 6. Full details of the μSR studies on this compound are reported in an accompanying paper [10]. This material has its main magnetic ordering transition around 33 K and behaves as an easy-plane AF at low fields. However, at higher fields it has a metamagnetic transition, switching from AF to FM behaviour [11]. This transition can be assigned to overcoming a weak AF interaction between the strongly FM-coupled bilayer units and it has been observed to take place for applied fields in the region of 50 G at temperatures well below the magnetic transition [11]. In the ZF μSR of this material in the magnetically ordered state there are two main precession components, corresponding at low temperatures to internal fields of $B_1 = 62$ and $B_2 = 121$ G with asymmetry amplitudes a_1 and a_2 [10]. Using this information, the expected field dependence of the total oscillation amplitude can then be calculated as a sum of two terms

$$a_{\text{static}}(B) = a_1 A_{\text{osc}}(b_1) + a_2 A_{\text{osc}}(b_2), \tag{24}$$

where $b_1 = B/B_1$, $b_2 = B/B_2$ and $A_{\text{osc}}(b)$ is given by (7). The measured total oscillation amplitude is shown in figure 6(a) along with the static prediction (24). The difference Δa between the measured amplitude and the static prediction is shown in figure 6(b). It can be seen that the asymmetry first starts to deviate from the static value above 15 G and between 15 and 40 G it falls faster than the static value, indicating that the internal field distribution is becoming more closely aligned with the applied field than in the static case. The main metamagnetic transition is revealed by the sharp increase in Δa above 50 G, indicating a significant change in the field distribution, this time producing an increased weighting of internal fields that are transverse to the applied field.

A simple model can be used to describe the spin transition as seen by the muons. In the polycrystalline sample it is assumed that the spins are constrained to lie in the easy plane of each crystallite and the transition occurs when the in-plane field component is greater than a threshold field B_c, which is assumed to be isotropic within the plane. Polycrystalline averaging

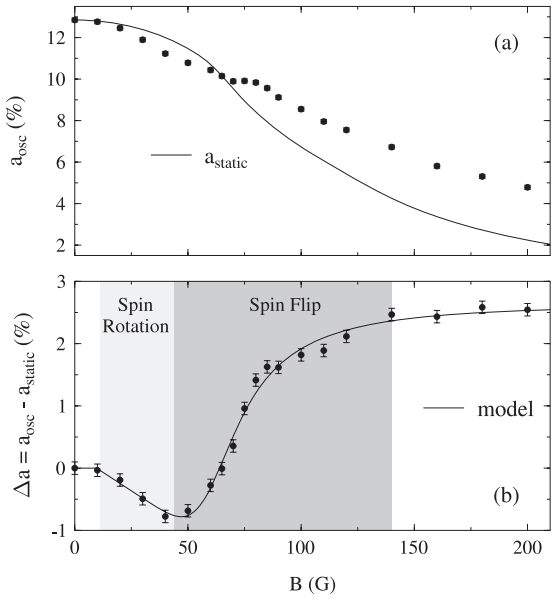

Figure 6. (a) Effect of a longitudinal field on the total amplitude of precession signal at 14 K in the layered magnet $CuW(CN)_8(tetrenH_5)_{0.8}\cdot 7H_2O$. The solid line shows the predicted field dependence (24) for a fixed spin distribution on the basis of the frequencies and amplitudes measured in zero field [10]. (b) The difference between the measured total precession amplitude and the static prediction. The solid line is the result of fitting to model (27), as described in the text. Regions are indicated where the changes in Δa are mainly due to spin rotation and mainly due to spin flip.

then leads to the following field-dependent function describing the fraction of the sample that is above the transition

$$\begin{aligned} f(B) &= 0 & B &< B_c \\ f(B) &= 1 - (B_c/B)^n & B &> B_c \end{aligned} \tag{25}$$

with $n = 2$ for this XY anisotropy model. If the anisotropy was of the Ising type, constraining the spins to lie in one direction within the plane, then the smaller value $n = 1$ would be expected, giving a more slowly rising function. In contrast, an ideal isotropic Heisenberg system would have a sharp transition corresponding to an infinite value for n. The contribution of non-flipped crystallites is important below B_c, and above a small threshold field B_t it gives a linear dependence representing spin rotation processes, i.e.

$$\begin{aligned} a_{rot}(B) &= 0 & B &< B_t, \\ a_{rot}(B) &= \alpha(B - B_t) & B &> B_t. \end{aligned} \tag{26}$$

The data of figure 6(b) are found to be well described by the sum of flipped and non-flipped (rotated) terms

$$\Delta a(B) = f(B)a_{flip} + (1 - f(B))a_{rot}(B). \tag{27}$$

Fitting the data to (27) gives the values $B_c = 56(1)$ G, $a_{flip} = 2.6(1)\%$ and $n = 3.4(4)$, with a Gaussian broadening of 12(3) G for $f(B)$ also being included in the fit. These parameters are consistent with the results obtained from direct magnetic measurements [10, 11] and with the dominance of easy-plane type spin constraints for this system.

4. Conclusion

In this study the internal magnetic field distribution seen by a muon probe implanted into a polycrystalline magnet has been investigated as a function of the applied magnetic field. The case of a rigid spin distribution has been considered in detail in both the LF and TF configurations. Expressions have been obtained in each case for the field dependence of the amplitudes of the precessing and non-precessing components of the relaxation function and the functional form of the precession field distribution, along with the first and second moments of the distribution. Appropriate relaxation functions can easily be computed from these distributions. These expressions provide a useful point of reference for muon studies in the more general situation of a magnet in which the spin distribution is not rigidly fixed to its zero field value, but, by various mechanisms, becomes significantly modified in response to the applied field. In this case, the changes in the field distribution are revealed as deviations from the static expressions. A particular application is the study of metamagnetic transitions. This has been illustrated with a specific experimental example of a system showing a low-field spin transition, which is clearly revealed in the field-dependent amplitude of the total muon spin precession signal. The example provides a good demonstration that oriented single crystal measurements are not always needed for the study of metamagnetic transitions and that valuable information can be extracted from the field-dependent study of polycrystalline samples using μSR. It is anticipated that the results of this work should be useful in further such studies of field-dependent magnetic transitions using muons.

Acknowledgments

The author wishes to thank T Wasiutyński, B Bałanda and P Zieliński for collaboration and discussions and for introducing him to the molecular magnetic system that stimulated this work.

References

[1] Dalmas P and Yaouanc A 1997 *J. Phys.: Condens. Matter* **9** 9113
[2] Heffner R H and Nagamine K (ed) 2004 *J. Phys.: Condens. Matter* **16** (Special issue on μSR)
[3] Barsov S G *et al* 1990 *Hyperfine Interact.* **64** 415
[4] Kornilov E I and Pomjakushin V Yu 1991 *Phys. Lett.* A **153** 364
[5] Larkin M I *et al* 2000 *Physics* B **289/290** 153
[6] Satooka J, Kojima Y, Miyata S, Suzuki K, Higemoto W, Nishiyama K and Nagamine K 2003 *Physica* B **326** 585
[7] Maruta G, Nishiyama K and Takeda S 2001 *Polyhedron* **20** 1185
[8] Pratt F L 1997 *Phil. Mag. Lett.* **75** 371
[9] Podgajny R, Korzeniak T, Bałanda M, Wasiutyński T, Errington W, Kemp T J, Alcock N W and Sieklucka B 2002 *Chem. Commun.* **2002** 1138
[10] Pratt F L, Zieliński P M, Bałanda M, Podgajny R, Wasiutyński T and Sieklucka B 2007 *J. Phys.: Condens. Matter* **19** 456208
[11] Bałanda M, Korzeniak T, Pełka R, Podgajny R, Rams M, Sieklucka B and Wasiutyński T 2005 *Solid State Sci.* **7** 1113